Journal of Molecular Catalysis A: Chemical 409 (2015) 171–182

Contents lists available at ScienceDirect

Journal of Molecular Catalysis A: Chemical

journal homepage: www.elsevier.com/locate/molcata

Cascade engineered synthesis of ethyl benzyl acetoacetate and methyl isobutyl ketone (MIBK) on novel multifunctional catalyst

Saurabh C. Patankar, Sanjay K. Dodiya, Ganapati D. Yadav*

Department of Chemical Engineering, Institute of Chemical Technology, Nathalal Parekh Marg, Matunga, Mumbai 400 019, India

ARTICLE INFO

Article history:
Received 17 January 2015
Received in revised form 15 August 2015
Accepted 17 August 2015
Available online 21 August 2015

Keywords:
Multifunctional catalyst
Knoevenagel condensation
Aldol condensation
Hydrogenation
Methyl isobutyl ketone
Ethyl benzyl acetoacetate
Selectivity engineering

ABSTRACT

A novel trifunctional catalyst with basic, acidic and metal sites was synthesized by nanocolloidal method and used in industrially important reactions. in the laboratory. The synthesized catalyst consisted of palladium and hydrotalcite supported on transition metal modified hexagonal mesoporous silica (HMS) and was characterized in virgin and reused states using a number of techniques such as elemental analysis, FTIR, NH_3- TPD, CO_2- TPD, H_2- TPR, XRD and BET surface area. The activity of particular catalytic site was engineered so that a desired reaction pathway was followed in spite of possibility of multiple series and parallel or complex reactions. One pot cascade engineered synthesis of ethyl benzyl acetoacetate from benzaldehyde and ethyl acetoacetate was studied in solvent free condition in a batch reactor. The effects of various parameters on the rates of reaction were analysed to establish instantaneous selectivity. Reaction mechanism and kinetic modelling was studied to validate the experimental results. The reaction follows Langmuir-Hinshelwood-Hougen-Watson mechanism involving weak adsorption of reactants and products. The apparent activation energy was found to be 13 kcal/mol and intrinsic kinetic constant 33 $cm^6\ mol^{-1}\ g_{cat}{}^{-1}\ s^{-1}$. This study was further extended to synthesis of methyl isobutyl ketone (MIBK) from acetone in solvent free condition. Similar experimental and theoretical analysis was done for MIBK synthesis for which the activation energy and intrinsic kinetic constant were found to be 12 kcal/mol and 4 $cm^6\ mol^{-1}\ g_{cat}{}^{-1}\ s^{-1}$, respectively.

1. Introduction

Catalysis is the most pivotal principle of Green Chemistry which inherently aims at reduction of waste, both of material and energy. The active sites on the catalyst can be tailored to give desired products from reactants while suppressing, either totally or to the maximum extent, any generation of by-products [1]. Chemical and allied industry is characterized by several processes involving complex (series and/or parallel) reaction networks in which the selectivity of the desired product is influenced by a number of parameters. There are examples of reactions where the same type of catalyst is used in a series of reactions where the intermediate is reacted with the reactant already present in the reactor or a different reagent is added subsequently wherein there is no need for separation of the intermediate. Our laboratory pioneered this concept in the case of industrially relevant phase transfer catalysis [2] for fenvalerate production and solid superacids [3] for bisphenol-A manufacture, wherein the same catalyst was used in a single reactor without separation of catalyst or purification stage. We studied, for instance, the synthesis of bisphenol-A using supported heteropoly-acids (HPA) as a sequel to the Hock process used to make phenol and acetone [3]. Cascade engineered multistep reactions along with complex multifunctional catalyst yields required process intensification at molecular level [4,5]. In cascade reactions the single event triggers the conversion of a starting material to a product that becomes the intermediate reactant for the next reaction resulting in cascade transformations [6]. These reactions also obviously reduce workup and save capital costs significantly. The multifunctional catalysts required for such reactions possess multi-functionality such as acid, base and metal sites. Reactions occur on these multiple sites in a concerted or sequential manner [7]. Various studies on organic synthesis using heterogeneous multifunctional catalysts have been reported earlier. To illustrate a few, a residue free catalytic process for production of nabumetone (anti-inflammatory agent) was achieved through a cascade reaction system using nanocrystalline magnesium oxide [8]. A multifunctional catalyst consisting of HPA and noble metal deposited on ceria zirconia

* Corresponding author. Fax: +91 22 3361 1002.
E-mail addresses: gdyadav@yahoo.com, gd.yadav@ictmumbai.edu.in (G.D. Yadav).

http://dx.doi.org/10.1016/j.molcata.2015.08.018
1381-1169/

Nomenclature

A	ethyl acetoacetate
B	benzaldehyde
C	ethyl-2-[hydroxyl(phenyl) methyl]-3-oxobutanoate
D	ethyl(2E)-2-benzylidene-3-oxobutanoate
E	hydrogen
F	ethyl benzyl acetoacetate
Y	water
I	acetone
J	4-hydroxy-4-methylpentan-2-one
K	4-methylpent-3-en-2-one
L	4-methylpentan-2-one (MIBK)
M	2,6-dimethylhept-2-en-4-one (DIBK)
N	2,6-dimethylheptan-4-one (DIBC)
O	propan-2-ol
S	instantaneous selectivity
W	catalyst loading (g_{cat} cm^{-3})
S_b	base site
S_a	acid site
S_m	metal site
$C_{A.Sb}$	concentration of ethyl acetoacetate on base sites (mol cm^{-3})
$C_{B.Sb}$	concentration of benzaldehyde on base sites (mol cm^{-3})
$C_{C.Sb}$	concentration of ethyl-2-[hyodroxyl(phenyl)methyl]-3-oxobutanoate on base sites (mol cm^{-3})
C_A	concentration of ethyl acetoacetate in bulk (mol cm^{-3})
C_B	concentration of benzaldehyde in bulk (mol cm^{-3})
C_C	concentration of ethyl-2-[hydroxyl(phenyl) methyl]-3-oxobutanoate in bulk (mol cm^{-3})
C_D	concentration of ethyl(2E)-2-benzelidene-3-oxobutanoate in bulk (mol cm^{-3})
C_E	concentration of hydrogen in bulk (mol cm^{-3})
C_F	concentration of ethyl benzyl acetoacetate in bulk (mol cm^{-3})
C_I	concentration of acetone in bulk (mol cm^{-3})
k_1	reaction rate constant for surface reaction of ethyl acetoacetate and benzaldehyde on base sites (cm^3 mol^{-1} s^{-1})
k_4	reaction rate constant for addition reaction of benzaldehyde on metal sites (cm^3 mol^{-1} s^{-1})
k_5	reaction rate constant for aldol condensation of acetone (cm^3 mol^{-1} s^{-1})
k_8	reaction rate constant for hydrogenation of acetone (cm^3 mol^{-} s^{-1})
K_A	adsorption constant of A (ethyl acetoacetate) on base sites (cm^3 mol^{-1})
K_{B1}	adsorption constant of B (benzaldehyde) on base sites (cm^3 mol^{-1})
K_{B2}	adsorption constant of B (benzaldehyde) on acid sites (cm^3 mol^{-1})
K_{C1}	adsorption constant of C (ethyl-2-[hydroxyl(phenyl) methyl]-3-oxobutanoate) on base sites (cm^3 mol^{-1})
K_{C2}	adsorption constant of C (ethyl-2-[hydroxyl(phenyl) methyl]-3-oxobutanoate) on acid sites (cm^3 mol^{-1})
K_D	adsorption constant of D (ethyl(2E)-2-benzelidene-3-oxobutanoate) on acid sites (cm^3 mol^{-1})
K_E	adsorption constant of E (hydrogen) on metal sites (cm^3 mol^{-1})
K_F	adsorption constant of F (ethyl benzyl acetoacetate) on metal sites (cm^3 mol^{-1})
K_{I1}	adsorption constant of I (acetone) on base sites (cm^3 mol^{-1})
K_{I2}	adsorption constant of I (acetone) on metal sites (cm^3 mol^{-1})
k'	apparent reaction rate constant for reaction of benzaldehyde and ethyl acetoacetate (cm^3 mol^{-1} s^{-1})
k"	apparent reaction rate constant for reaction of acetone (cm^3 mol^{-1} s^{-1})
k	intrinsic kinetic constant (cm^6 mol^{-1} $g_{cat}{}^{-1}$ s^{-1})
C_{Sb}	concentration of vacant base catalytic sites (mol cm^{-3})
C_{Sa}	concentration of vacant acid catalytic sites (mol cm^{-3})
C_{Sm}	concentration of vacant metal catalytic sites (mol cm^{-3})
C_{tb}	total concentration of base sites (mol cm^{-3})
C_{ta}	total concentration of acid sites (mol cm^{-3})
X_A	fractional conversion of ethyl acetoacetate
X_I	fractional conversion of acetone

mixed oxide for de-NO_x processes has been developed [9]. The α-alkylation of various nitriles with carbonyl compounds has been reported using hydrotalcite supported palladium nanoparticles as multifunctional catalyst [10]. The synthesis of multifunctional mesoporous catalysts containing multiple site isolated functional groups has been achieved for selective catalysis of hydrophilic and hydrophobic reactants in Henry's reaction [11]. One pot synthesis of quinolines from 2-amino benzyl alcohol and various carbonyl compounds using ruthenium grafted hydrotalcite have been reported [12]. Recently we have provided an in-depth analysis of different cascade engineered reactions such as selective synthesis of γ-butyrolactone from succinic acid using supported palladium-copper on alumina xerogel catalyst and isopropyl alcohol as solvent [13,14], and synthesis of γ-valerolactone, 1,4-pentanediol and 2-methyltetrahydrofuran from levulinic acid using novel Pd-Cu/ZrO_2 catalyst in water as solvent [15].

In the current work, selectivity engineering principles have been applied to a complex reaction network using a tri-functional catalyst with base, acid and metal sites. A new catalyst is developed by nanocolloidal method and used in industrially important reactions. Two examples have been meticulously studied. The first involves the reaction between benzaldehyde and ethyl acetoacetate in solvent less condition, which proceeds through multiple series and parallel reactions occurring on base, acid and metal catalytic sites. The desired product is ethyl benzyl acetoacetate which is used as a flavoring agent. There is no information in open literature on the selective synthesis of ethyl benzyl acetoacetate starting from benzaldehyde and ethyl acetoacetate in a single pot. A theoretical model was conceived and tested against experimental data. The theory was further extended to reaction of acetone in solvent less condition to yield methyl isobutyl ketone (MIBK). All results are novel and can be extended to different catalytic reactions.

2. Experimental

2.1. Chemicals

Palladium nitrate [Pd $(NO_3)_2{\cdot}2H_2O$] was procured from M/s Otto Kemi Ltd., Mumbai, India. Ethanol, magnesium nitrate [$Mg(NO_3)_2{\cdot}6H_2O$], aluminum nitrate [$Al(NO_3)_2{\cdot}9H_2O$], sodium hydroxide, sodium citrate [$Na_3(C_6O_7H_3)$], 35% w/w ammonium

hydroxide [NH_4OH], 35% w/w aqueous hydrochloric acid, mesitylene and hexadecylamine were procured from M/s S.D. Fine Chemical Ltd., Mumbai. Tetraethyl orthosilicate (TEOS) and titanium isopropoxide [Ti(*iso*$OC_3H_7)_4$] were procured from M/s Merck Chemicals Ltd., and M/s Spectrochem Ltd., Mumbai, respectively.

2.2. Catalyst preparation

Titanium modified hexagonal mesoporous silica (HMS), designated as HMS (Ti), and was prepared as reported earlier [16]. Hexadecylamine was used supramolecular template/surfactant and mesitylene was used as pore expander. The process of calcination was necessary to remove the organic template. Molar ratios of SiO_2/swelling agent = 1.66 and swelling agent/surfactant = 2.33 were applied for the preparation of HMS (Ti). Required amount of HMS (Ti) was then added to aqueous solution of magnesium nitrate [$Mg(NO_3)_2{\cdot}6H_2O$] and aluminum nitrate [$Al(NO_3)_3{\cdot}9H_2O$]. The quantities of magnesium nitrate and aluminum nitrate were fixed such that the Mg/Al molar ratio was 2:1. The mass ratio of calcined hydrotalcite (CHT):HMS (Ti) was fixed at 2:10. The resulting solution was stirred vigorously for 30 min at 60 °C to form slurry. The slurry was added drop-wise to 35% (w/w) aqueous ammonium hydroxide [NH_4OH] under vigorous stirring while maintaining pH at 9–10. The slurry was aged at 90 °C for 3 h. The precipitate was filtered off and put into a container of distilled water for decantation. The decanted precipitate was recovered by filtration and dried at 100 °C for 2 h in oven. This served as the host structure for loading palladium by nanocolloidal method. The colloidal palladium suspension of particles was obtained by hydrolysis of aqueous solution of palladium nitrate [$Pd(NO_3)_2{\cdot}2H_2O$] and sodium citrate [$Na_3(C_6O_7H_3)$] with 0.5 M NaOH. The molar ratio of [citrate]/[Pd] was 1. The exchange process of the host structure was performed in air at room temperature for 12 h. The required amount of host structure was dispersed in the required amount of 0.003 M aqueous suspension of colloid Pd-hydroxy citrate particles. The Pd-colloid-Mg/Al/HMS(Ti)-layered double hydroxide was then recovered and washed by dispersion and centrifugation in deionized water and then dried at 80 °C for 4 h. The final catalyst was obtained by calcination at 500 °C in air for 3 h. The prepared catalyst consisted of palladium loaded on calcined hydrotalcite which was supported on titanium modified hexagonal mesoporous silica. The catalyst was also made by sol–gel and impregnation methods. A series of catalysts designated as xPd-CH-Z were prepared, where *x*% w/w loading of palladium (Pd), calcined hydrotalcite supported on titanium modified hexagonal mesoporous silica (CH) and *Z* is the method of synthesis (Z = N, S or I; N = nanocolloidal, S = sol–gel, I = impregnation).

2.3. Catalyst characterization

Temperature programmed desorption (TPD) using NH_3 and CO_2 as probe molecules was used for acidity and basicity measurement, respectively (Autochem II 2910, Micromeritics, USA) to understand the nature of active sites generated on the catalyst surface. For NH_3–TPD runs, the catalyst sample was degassed under nitrogen flow upto 300 °C in a quartz tube. Ammonia in helium (5% v/v) was adsorbed on the catalyst at room temperature. The physisorbed gas was then removed by flow of nitrogen. Chemisorbed ammonia was measured using TPD in conjunction with TCD detector. Similar procedure was followed for CO_2–TPD measurements using 10% v/v carbon dioxide in helium gas. The TPR study was performed using H_2 as probe molecule. Powder XRD (MinislexRegako, Japan) was used to study the multifunctional nature of catalyst with Cu Kα radiation with beam current of 40 kV and 100 mA. The data were collected by varying 2θ from 0–80°. Infrared spectra of the samples pressed in KBr pellets were obtained at a resolution of 2 cm^{-1} between 4000 cm^{-1} and 400 cm^{-1}. The surface properties of catalyst prepared were measured by the Brunauer–Emmett–Teller (BET) method by using ASAP 2010 (Micromeritics, USA) instrument. The catalyst samples were first degassed under vacuum at 350 °C for 4 h. The measurements were made at liquid nitrogen temperature using N_2 gas as the adsorbent with a multipoint method. Micrographs of surface morphology of the catalyst samples were captured with Camera SU 30 microscope, JEOL, Japan equipment. The samples were mounted on specimen studs and coated with platinum by sputtering to prevent charring of samples during analysis.

2.4. Reaction procedure and analysis

All experiments for synthesis of ethyl benzyl acetoacetate and MIBK were carried out in a batch autoclave (Amar Equipments, Mumbai) of 100 mL capacity. The reactor was equipped with four blade 45° inclined pitched turbine impeller, temperature controller (±1 °C), pressure indicator and speed regulator (±5 rpm). Reactants and the catalyst were charged into the reactor. The reaction mixture was flushed with nitrogen to remove traces of air, pressurized with hydrogen to 5 atm and then heated to the desired temperature. In a standard reaction for synthesis of ethyl benzyl acetoacetate, equimolar quantities of benzaldehyde and ethylacetoacetate were used in such a way that the reaction mixture was 35 cm^3 with *n*-decane as internal standard. For MIBK synthesis, 30 mL acetone was used with *n*-decane as internal standard. Samples were withdrawn periodically after the desired temperature had reached and were analyzed using GC equipped with a capillary column BP-50 (0.25 μm film thickness × 0.25 mm column ID × 25 m column length) and FID detector. The products were confirmed by GC–MS (QP2010, Shimadzu) and by matching the residence time of pure samples.

3. Results and discussion

3.1. Efficacy of various catalysts

A variety of catalysts synthesized in the laboratory, according to a well thought strategy, were evaluated for their efficacy and robustness in the synthesis of twoindustrially relevant and academically interesting compounds, namely, ethyl benzyl acetoacetate and MIBK synthesis. The strategy behind studying these two reactions was to understand the relative rates of condensation, dehydration and hydrogenation and thereby to design and synthesize a suitable trifunctional catalyst which will give maximum selectivity of the desired products. In the case of formation of ethyl benzyl acetoacetate, the aldehyde and ester react whereas in the case of MIBK synthesis, there is a self-condensation of acetone. Thus, the relative strength of basic, acidic and metal sites could be tuned properly. Table 1 lists the various catalysts prepared by different methods having different site densities, distribution and strengths of Pd, MgO and Al_2O_3. The catalyst made by impregnation method was not found to give high selectivity towards ethyl benzyl acetoacetate and MIBK. The catalyst made by nanocolloidal method had a comparable activity and selectivity towards ethyl benzyl acetoacetate and MIBK with the catalyst made by sol–gel method. However, the catalyst made by nanocolloidal method was found to be reusable as the active phase in the catalyst made by sol–gel method leached in reaction mixture on reuse (Tables ES1 and ES2). Hence further studies were done with the catalyst made by nanocolloidal method. The loading of palladium determines the catalytic strength of metal sites and the Mg/Al ratio decides the distribution of the catalytic strength of base and acid catalytic sites. In the case of ethyl benzyl acetoacetate synthesis, increasing

Table 1
Comparison of different catalysts for ethyl benzyl acetoacetate and MIBK synthesis.

Catalyst	Method of synthesis	Mg/Al ratio	Reaction 1[a]		Reaction 2[b]	
			Conversion (%) of ethyl acetoacetate	Selectivity towards ethyl benzyl acetoacetate	Conversion (%) of acetone	Selectivity towards MIBK
0.2Pd-CH(2:1)-N	Nanocolloids	2:1	38	75	16	100
0.2Pd-CH(2:1)-S	Sol–gel	2:1	33	78	13	95
0.2Pd-CH(2:1)-I	Impregnation	2:1	32	61	9	82
1Pd-CH(2:1)-N	Nano colloids	2:1	42	60	8	85
0.05Pd-CH(2:1)-N	Nano colloids	2:1	39	86	10	100
0.2Pd-CH(3:1)-N	Nano colloids	3:1	34	78	16	100
0.2Pd-CH(1:2)-N	Nano colloids	1:2	20	65	9	78

Reaction conditions:
[a]Ethyl acetoacetate:, benzaldehyde: 0.15 mol, speed of agitation: 10000.133 mol rpm, catalyst: 0.065 g, temperature: 413 K, time: 30 min, organic phase volume: 32.7 cm^3, catalyst loading: 1.978×10^{-3} g cm^{-3}.
[b]Acetone: 0.4 mol, volume = 30 cm^3, speed of agitation: 1000 rpm, catalyst loading: 0.06 g, temperature: 463 K, time: 30 min.

the palladium loading to 1% (w/w) accelerated hydrogenation of benzaldehyde and hence resulted in lower selectivity of 60%. The lowering of the palladium loading to 0.05% (w/w) from 0.2% (w/w) stopped the side reaction of hydrogenation of benzaldehyde and resulted in enhancement in selectivity to 86% from 75%. However, conversion of ethyl acetoacetate remained the same as the desired reaction pathway involves base and acid catalyzed reactions as first two steps. In 0.2Pd-CH(2:1)-N, the change in Mg/Al ratio to 3:1 resulted in reduction of the acid site strength and thus a lower conversion (34%) was obtained since the rate of dehydration reaction had correspondingly decreased. Selectivity towards ethyl benzyl acetoacetate remained the same as the side reaction is metal catalyzed and metal strength was unaffected by the change in Mg/Al ratio. The decrease in Mg/Al ratio to 1:2 resulted in slower rate of Knoevenagel condensation reaction due to decrease in base site strength leading to lower conversion of ethyl acetoacetate (20%) as benzaldehyde gets utilized in the parallel reaction of hydrogenation on metal sites. It thus decreased selectivity towards ethyl benzyl acetoacetate to 65%. In the case of MIBK synthesis, lowering the palladium loading did not affect the selectivity as 100% selectivity was achieved even with 0.2% (w/w) palladium loading. However, increase in palladium loading to 1% (w/w) resulted in increased rate of side reaction of hydrogenation of acetone and hence resulted in decreased selectivity of 85% towards MIBK. The decrease in Mg/Al ratio to 1:2 resulted in slower aldol condensation rate and hence increased the rate of hydrogenation of acetone which caused lower selectivity of 78% towards MIBK. 0.2Pd-CH(2:1)-N catalyst was observed to give the best results in the complex network of series and parallel reactions with similar controlling mechanisms in both ethyl benzyl acetoacetate and MIBK syntheses and hence was studied in detail. Its full characterization is presented here. In this catalyst HMS is ~85% by wt. A detailed theoretical analysis of both the chemistries is described later.

3.2. Catalyst characterization

3.2.1. Temperature programmed desorption (TPD) and temperature programmed reduction (TPR)

The total acidity and basicity of catalyst was found to be 0.30 mmol/g_{cat} NH_3 and 0.321 mmol/g_{cat} CO_2, respectively. Fig. 1a shows the reduction peak centred at ~400 °C confirming the presence of active metal sites on the catalyst surface. In Fig. 1b the two peaks at 140 and 450 °C shown in red correspond to intermediate and strong basic sites. The single peak in temperature range 70–170 °C shown in blue corresponds to weak acid sites.

3.2.2. X-ray diffraction

A single significant peak at 2θ value 25° with a d-value 2.35 is given for the catalyst. No sharp peaks were observed because of amorphous nature of support as well as of the prepared multifunctional catalyst. Since the quantities of hydrotalcite and palladium metal were quite less as compared to the support HMS (~85%), XRD pattern does not show any peaks due to Pd, Mg, and Al in the catalyst.

3.2.3. FTIR

Fig. 2 shows the spectra for HMS(Ti) [A] and 0.2Pd-CH(2:1)-N [B]. The absorption at 1088 cm^{-1} with shoulders is attributed to asymmetric stretching of Si—O—Si for HMS(Ti). The band at 466.08 cm^{-1} is given by SiO_4 tetrahedral orientation. The band at 3450 cm^{-1} is attributed to hydrogen bonded hydroxyl groups with corresponding deformation mode (δ HOH) at 1635 cm^{-1}. There are no characteristic peaks observed for aliphatic C—H stretching vibrations and C—H bonding which confirm removal of template after calcination of catalyst.

3.2.4. BET surface area measurement

Hysteresis loops shown in the isotherms confirm the mesoporous nature of different catalysts. From isotherms of HMS and HMS(Ti) in Fig. 3a and b, respectively, it can be concluded that incorporation of hetero-element enhances the mesoporosity of the support. Also from Table 2, it is observed that the surface areas of catalysts were reduced after incorporation of titanium and palladium metal on support, but the average pore diameter had increased. Analysis of used catalyst showed that the average pore diameter has further increased due to possible clogging of small pores during reaction.

3.2.5. Scanning electron microscopy

Micrographs of HMS and HMS(Ti) at resolution of 1000 showed that the modification of support by heteroatom did not affect the overall morphology. The image of 0.2Pd-CH(2:1)-N catalyst at resolution of 5000 shows the nature of nanoparticles (Fig. ES1). Further, the energy dispersive X-ray spectroscopy (EDAX) analysis of used catalyst showed retention of all metal species on the catalyst.

3.3. Theoretical aspects of selectivity engineered cascade chemistry

The possible reactions of benzaldehyde and ethyl acetoacetate on PCH(Ti)N catalyst are listed in Scheme 1. With reference to Scheme 1, three reactions occur sequentially to yield ethyl benzyl acetoacetate, namely: (i) base catalyzed Knoevenagel condensation of ethylacetoacetate (A) and benzaldehyde (B) to form ethyl

Table 2
Textural properties of virgin and reused catalysts and supports.

Textural characteristic	HMS	HMS (Ti)	0.2Pd-CH(2:1)-N (virgin)	0.2Pd-CH(2:1)-N (reused)
Surface area (m^2/g)	585	559	475	312
Pore volume (cm^3/g)	0.36	0.46	0.87	1.29
Pore diameter (nm)	3	3.2	8.6	17

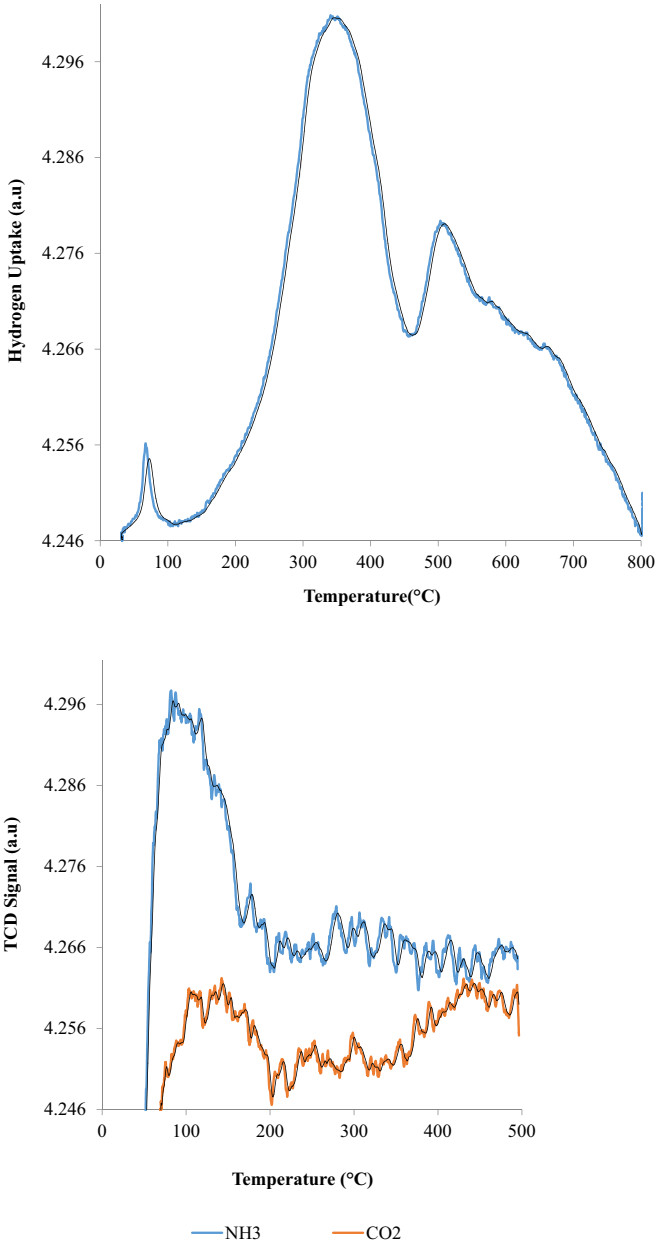

Fig. 1. (a) TPR profile of 0.2Pd-CH(2:1)-N, (b) TPD-NH_3 and TPD-CO_2 profiles of 0.2Pd-CH (2:1)-N.

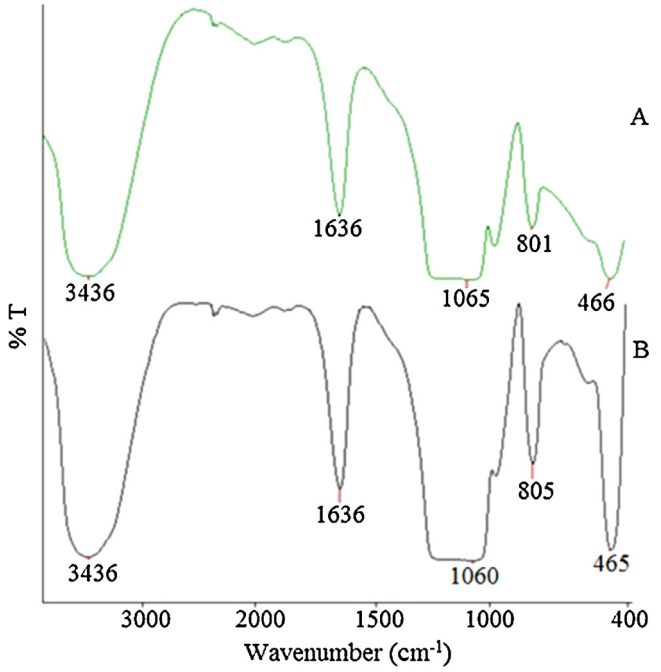

Fig. 2. FTIR spectra of HMS(Ti) [A] and 0.2Pd-CH(2:1)-N [B].

2-[hydroxyl(phenyl)methyl]-3-oxobutanoate (C) (Reaction a), (ii) acid catalyzed dehydration of the condensation product to form ethyl (2E)-2-benzylidene-3-oxobutanoate (Reaction b), and (iii) its further hydrogenation on metal site to form ethyl benzyl acetoacetate (ethyl-2-benzyl-3-oxobutanoate) (Reaction c). In this synthetic route, hydrogen does not participate in Reactions (a) and (b). The desired sequence of steps was obtained by tuning the catalyst activity in such a manner that the base sites were of the highest activity followed by the acid sites and then the metal sites. The tuning of the catalyst could be done by adjusting the loading of active species on the catalyst support. In these three consecutive steps, the first step of Knoevenagel condensation is the rate determining step which was ascertained by performing the reaction both in the presence and the absence of hydrogen.

In the presence of hydrogen, the final product of ethyl benzyl acetoacetate is the sole product. Without hydrogen, ethyl(2E)-2-benzylidene-3-oxobutanoate was the sole product which was obtained by Knoevenagel condensation and subsequent dehydration. The consecutive reactions of dehydration and hydrogenation occur as soon as the Knoevenagel condensation product is formed. The reactant concentration with respect to catalyst active site strength for acid catalyzed dehydration and metal catalyzed hydrogenation remains lower than the base catalyzed reaction. The rate determining step was the base catalyzed Knoevenagel condensation reaction. Apart from the desired sequence of the Reactions (a–c); parallel reaction of dimerization of benzaldehyde to form benzyl benzoate (Reaction d) on acid site and hydrogenation of benzaldehyde on metal site to form benzyl alcohol (Reaction e) were observed on 0.2PCH(Ti)N. The formation of benzyl alcohol by hydrogenation of benzaldehyde was completely suppressed by adjusting the loading of palladium to 0.05% (w/w) and thus altering the metal site activity. However, the dimerization of benzaldehyde occurred on acid site. The formation of benzyl benzoate increased in reaction mixture with time as the concentration of ethyl acetoacetate decreased. There was hence a need to find out the dependent parameters and constants for instantaneous selectivity of ethyl benzyl acetoacetate. To derive the rate equation, following steps were assumed: Benzaldehyde (B) adsorbs on base site (S_b)

$$B + S_b \overset{K_{B1}}{\Leftrightarrow} B \times S_b \quad (1)$$

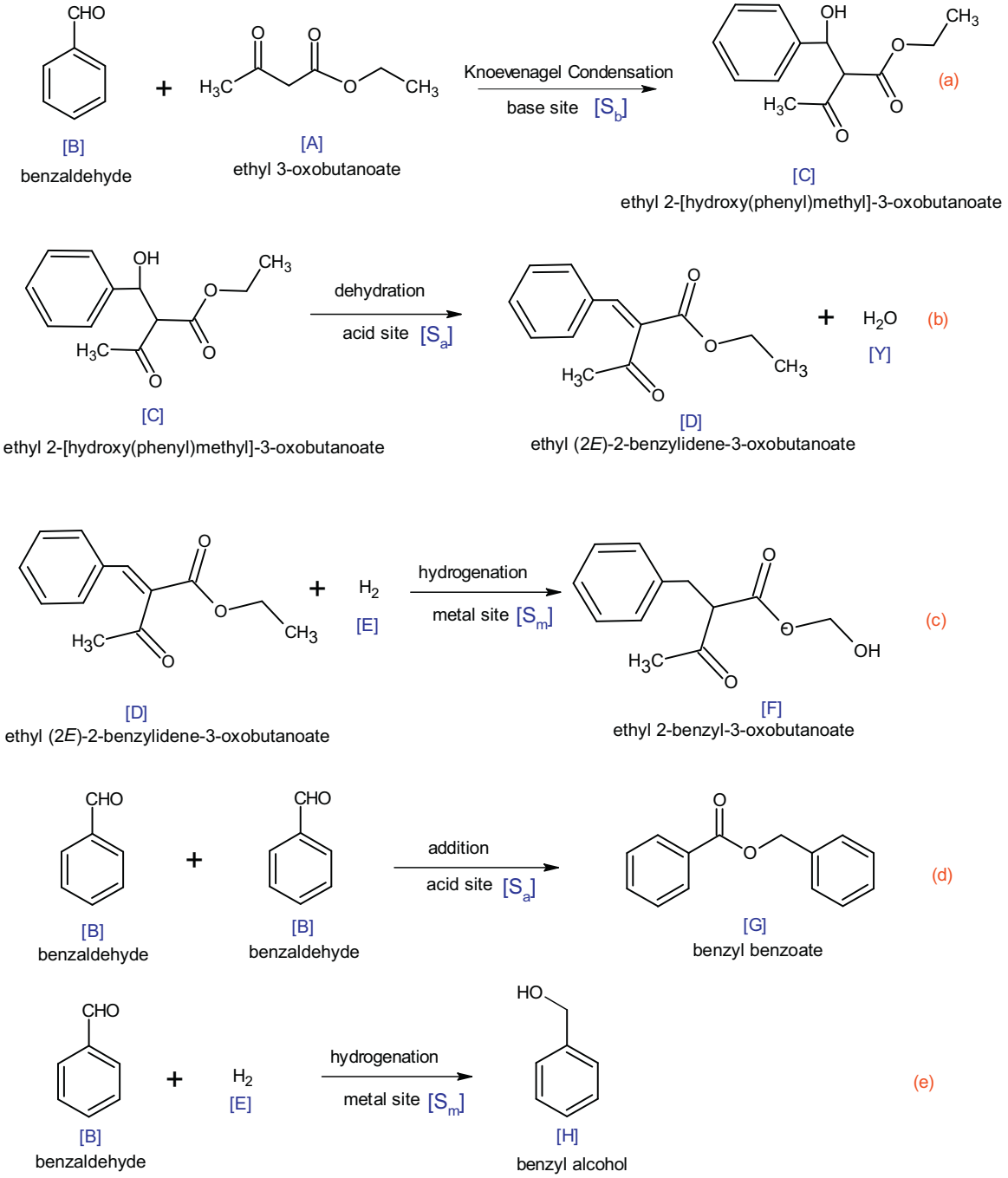

Scheme 1. Reaction of benzaldehyde and ethyl acetoacetate on 0.2Pd-CH(2:1)-N catalyst in presence of hydrogen.

Ethyl acetoacetate (A) adsorbs on base site (S_b)

$$A + S_b \overset{K_A}{\leftrightarrow} A \times S_b \quad (2)$$

Knoevenagel condensation of adsorbed benzahdehyde and ethyl acetoacetate

$$A \times S_b + B \times S_b \overset{k_1}{\rightarrow} C \times S_b + S_b \quad (3)$$

Desorption of condensation product ethyl-2-[hydroxyl (phenyl)methyl]-3-oxobutanoate from base site

$$C \times S_b \overset{1/K_{C1}}{\leftrightarrow} C + S_b \quad (4)$$

Adsorption of the condensation product on acid site (S_a)

$$C + S_a \overset{K_{C2}}{\leftrightarrow} C \times S_a \quad (5)$$

Dehydration reaction on acid site

$$C \times S_a \overset{k_2}{\rightarrow} D \times S_a + Y \quad (6)$$

Desorption of dehydration reaction product ethyl(2E)-2-benzylidene-3-oxobutanoate from acid site

$$D \times S_a \overset{1/K_{D1}}{\leftrightarrow} D + S_a \quad (7)$$

Adsorption of dehydration product on metal site (S_m)

$$D + S_m \overset{K_{D2}}{\leftrightarrow} D \times S_m \quad (8)$$

Dissociative adsorption of hydrogen on metal site

$$E + 2S_m \overset{K_E}{\leftrightarrow} 2\sqrt{E} \times S_m \quad (9)$$

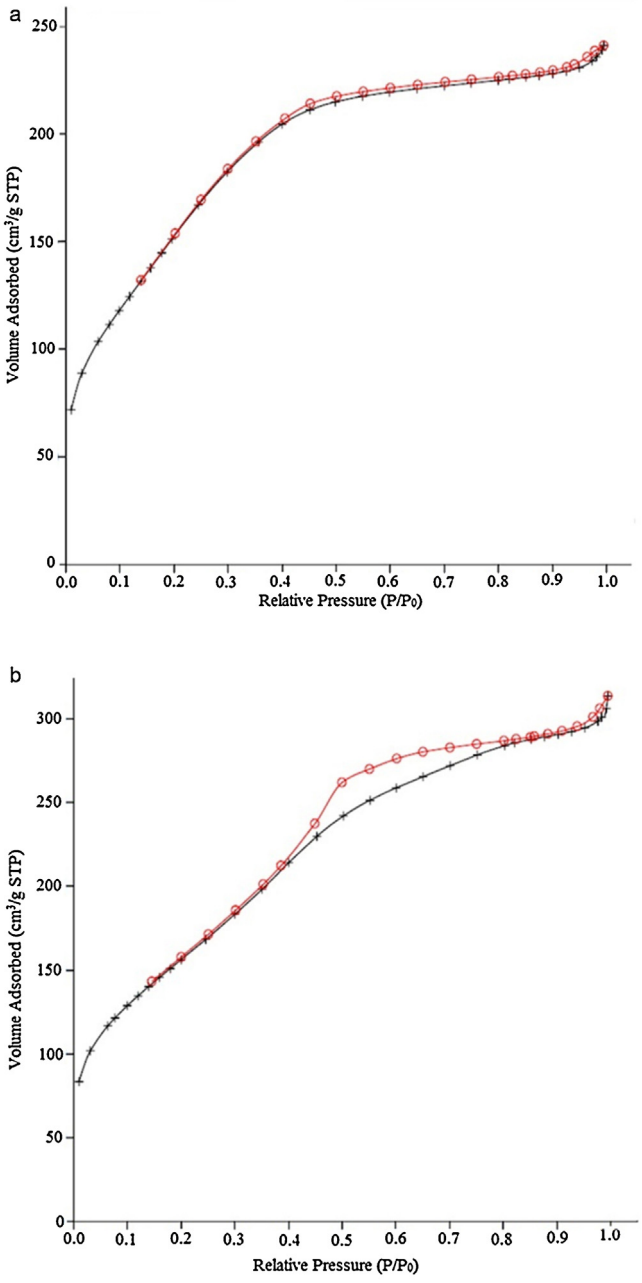

Fig. 3. (a) BET adsorption–desorption isotherm of HMS, (b) BET adsorption–desorption isotherm of HMS(Ti).

Hydrogenation reaction on metal site

$$D \times S_m + \sqrt{E} \times S_m \xrightarrow{k_3} F \times S_m + S_m \quad (10)$$

Desorption of product ethyl benzyl acetoacetate from metal site

$$F \cdot S_m \overset{1/K_F}{\leftrightarrow} F + S_m \quad (11)$$

Adsorption of benzaldehyde on acid site (S_a)

$$B + S_a \overset{K_{B2}}{\leftrightarrow} B \times S_a \quad (12)$$

Addition reaction of benzaldehyde on acid site

$$B \times S_a + B \times S_a \xrightarrow{k_4} G \times S_a + S_a \quad (13)$$

Desorption of addition product benzyl benzoate from acid site

$$G \times S_a \overset{1/K_G}{\leftrightarrow} G + S_a \quad (14)$$

As step (3) is the rate determining step, following correlations are obtained.

$$C_{B\times Sb} = K_{B1} C_B C_{Sb} \quad (15)$$

$$C_{A\times Sb} = K_A C_A C_{Sb} \quad (16)$$

$$C_{C\times Sb} = K_{C1} C_C C_{Sb} \quad (17)$$

$$C_{C\times Sa} = K_{C2} C_C C_{Sa} \quad (18)$$

$$C_{D\times Sa} = K_{D2} C_D C_{Sa} \quad (19)$$

$$C_{B\times Sa} = K_{B2} C_B C_{Sa} \quad (20)$$

The instantaneous selectivity can be represented as:

$$S_{F/G} = \frac{\frac{dC_F}{dt}}{\frac{dC_G}{dt}} \quad (21)$$

$$S_{F/G} = \frac{k_1 C_{A\times Sb} C_{B\times Sa}}{k_4 C_{B\times Sa}^2} \quad (22)$$

Substituting the Eq. (16), Eqs. (15) and (20) in Eq. (22),

$$S_{F/G} = \frac{k_1 K_A K_{B1} C_A C_{Sb}^2}{k_4 K_{B2} C_B C_{Sa}^2} \quad (23)$$

Site balance of base sites yield following:

$$C_{tb} = C_{A\times Sb} + C_{B\times Sb} + C_{C\times Sb} + C_{Sb} \quad (24)$$

$$C_{Sb} = \frac{C_{tb}}{[1 + K_A C_A + K_{B1} C_B + K_{C1} C_C]} \quad (25)$$

Site balance of acid sites yield following:

$$C_{ta} = C_{C\times Sa} + C_{D\times Sa} + C_{Sa} \quad (26)$$

$$C_{Sa} = \frac{C_{ta}}{[1 + K_{C2} C_C + K_{D1} C_D]} \quad (27)$$

Substituting Eqs. (27), (25) and in Eq. (23),

$$S_{F/G} = \frac{k_1 K_A K_{B1} C_A}{k_4 K_{B2} C_B (1 + K_A C_A + K_{B1} C_B)^2} \quad (28)$$

The constants were found from experimental data by interpolation (Table 3).

A plot of change in selectivity with time and comparison of theoretical values of selectivity and conversion of benzaldehyde and ethyl acetoacetate with experimental values is shown in Fig. 4.

The selective synthesis of ethyl benzyl acetoacetate involves steps 1–11 mentioned above. These can be pictorially described as given in Scheme 2.

It was assumed that surface reaction controls the rate of reaction. In this case considering the initial rate of reaction, a standard derivation was done and an equation for rate of reaction of A was derived:

$$-r_A = -\frac{dC_A}{dt} = k_1 C_{A\times S_b} C_{B\times S_b} - k'_1 C_{C\times S_b} C_{S_b} \quad (29)$$

$$-\frac{dC_A}{dt} = \frac{\left\{[k_1 K_A K_{B_1} C_A C_B - k'_1 K_{C_1} C_C] C_{tb}^2\right\}}{\left\{1 + K_A C_A + K_{B_1} C_B + K_{C_1} C_C\right\}^2} \quad (30)$$

When the reaction is far away from equilibrium, i.e., for initial rate of reaction;

$$-\frac{dC_A}{dt} = \frac{kWC_A C_B}{\left\{1 + K_A C_A + K_{B1} C_B\right\}^2} \quad (31)$$

where $kW = k_1 K_A K_{B_1} C_{tb}^2$ (32).W is the catalyst loading in g/cm^3. Substituting the values of adsorption constants shows that the term $\left\{1 + K_A C_A + K_{B1} C_B\right\}^2$ reduces to one as,

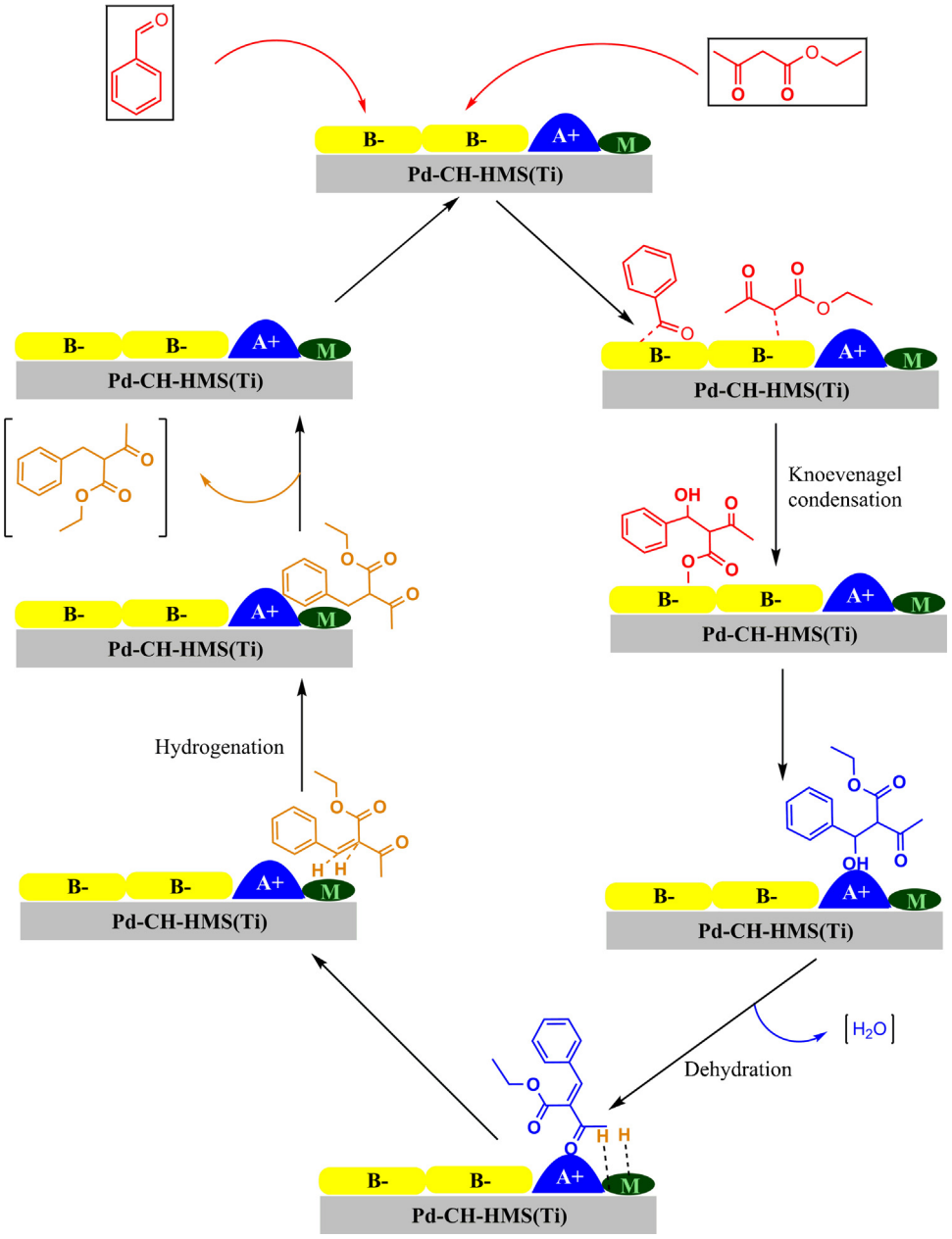

Scheme 2. Mechanism of selective synthesis of ethyl benzyl acetoacetate on 0.05Pd-CH(2:1)-N catalyst.

$$K_A C_A = 8.54 \times 10^{-4} \times 1.53 \times 10^{-2} = 1.31 \times 10^{-5}$$

$$K_{B1} C_B = 7.08 \times 10^{-4} \times 1.53 \times 10^{-2} = 1.08 \times 10^{-5}$$

$$1 + K_A C_A + K_{B1} C_B = 1 + 1.31 \times 10^{-5} + 1.08 \times 10^{-5} = 1$$

Thus Eq. (31) reduces to,

$$-\frac{dC_A}{dt} = kWC_A C_B \quad (33)$$

Let $\frac{C_{B_0}}{C_{A_0}} = M$ be the molar ratio of benzaldehyde to ethyl acetoacetate at time $t = 0$. Then the Eq. (33) can be written in terms of fractional conversion as,

$$\frac{dX_A}{dt} = kWC_{A_0}(1 - X_A)(M - X_A) = k'C_{A_0}(1 - X_A)(M - X_A) \quad (34)$$

when $M = 1$, Eq. (34) upon integration gives,

$$\frac{X_A}{(1 - X_A)} = k'C_{A0}t \quad (35)$$

3.4. Experimental aspects of cascade chemistry

3.4.1. Proof of absence of external mass transfer and pore diffusion resistance

The reactions were carried out at different agitation speed from 800 to 1000 rpm. No increase in the rate of reaction was observed beyond 1000 rpm thus indicating absence of external mass transfer resistance. If the Wiesz-Prater modulus (C_{wp}) for given catalyst is far less than unity then pore diffusion resistance is absent and reaction said to be kinetically controlled. Approximate particle size was measured by SEM images of catalyst as well as support. Average particle radius of catalyst was found to be 0.5 μm. An average pore radius was found to be 4 nm. Assuming tortuosity as 4 for

Table 3
Rate and adsorption constants for ethyl benzyl acetoacetate synthesis.

Parameter	Step	Value
$k_1 \times 10^2$ (cm^3 mol^{-1} s^{-1})	Knoevenagel condensation reaction constant	6.54
$k \times 10^2$ (cm^3 mol^{-1} s^{-1})	Addition reaction rate constant	1.99
$K_A \times 10^4$(cm^3 mol^{-1})	Adsorption constant of ethyl acetoacetate for base site	8.54
$K_{B1} \times 10^4$(cm^3 mol^{-1})	Adsorption constant of benzaldehyde for base site	7.08
$K_{B2} \times 10^7$(cm^3 mol^{-1})	Adsorption constant of benzaldehyde for acid site	9.02

the catalyst, an effective diffusivity of 7.5684×10^{-9} m^2/s was calculated [20]. Using all the calculated parameters and observed reaction rates, Wiesz-Prater moduli were calculated. Since all values of Wiesz-Prater moduli remained far less than unity throughout the reaction, it was concluded that there was no pore diffusion resistance and reactions are kinetically controlled.

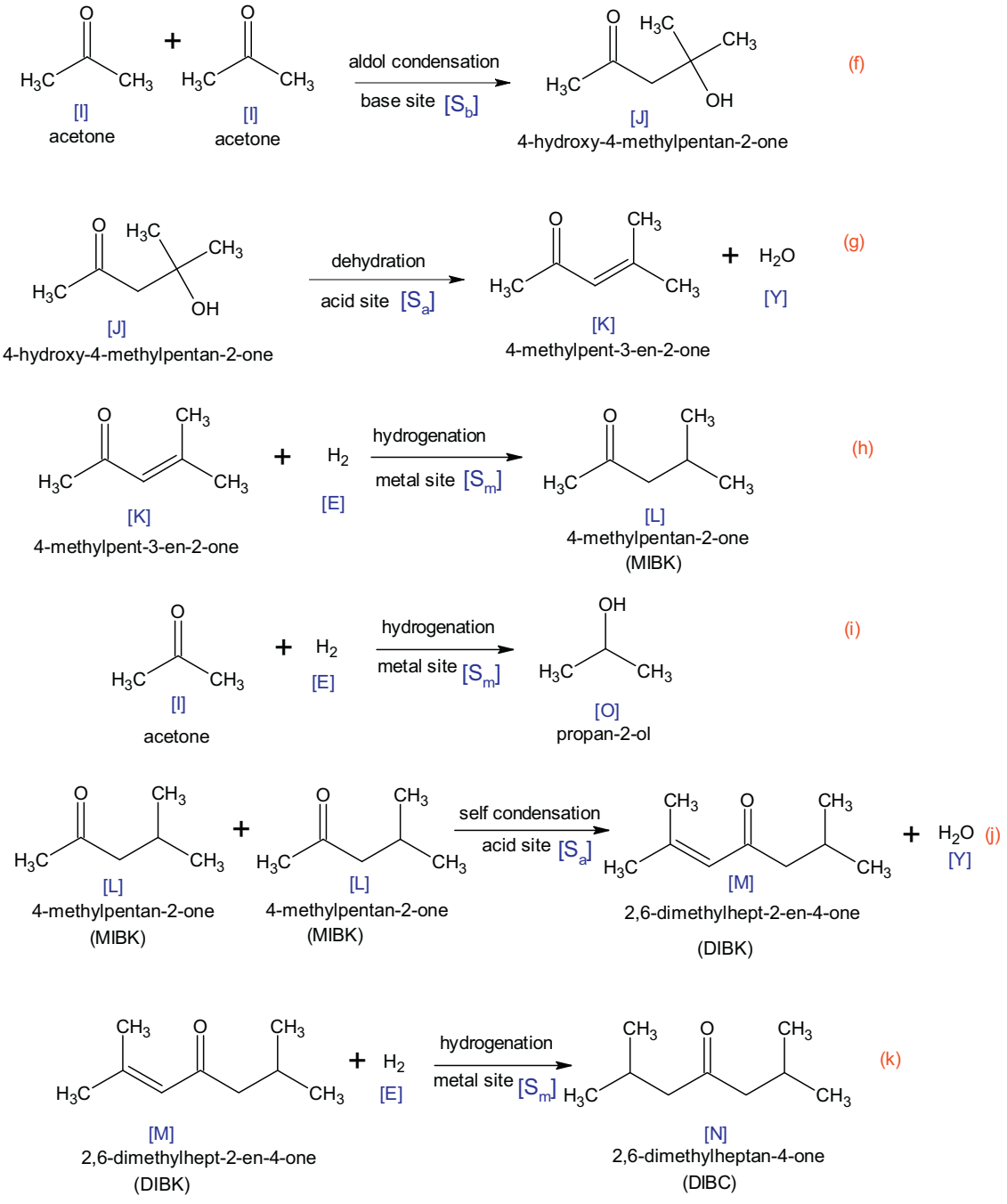

Scheme 3. Reaction of acetone on 0.2Pd-CH(2:1)-N catalyst in presence of hydrogen.

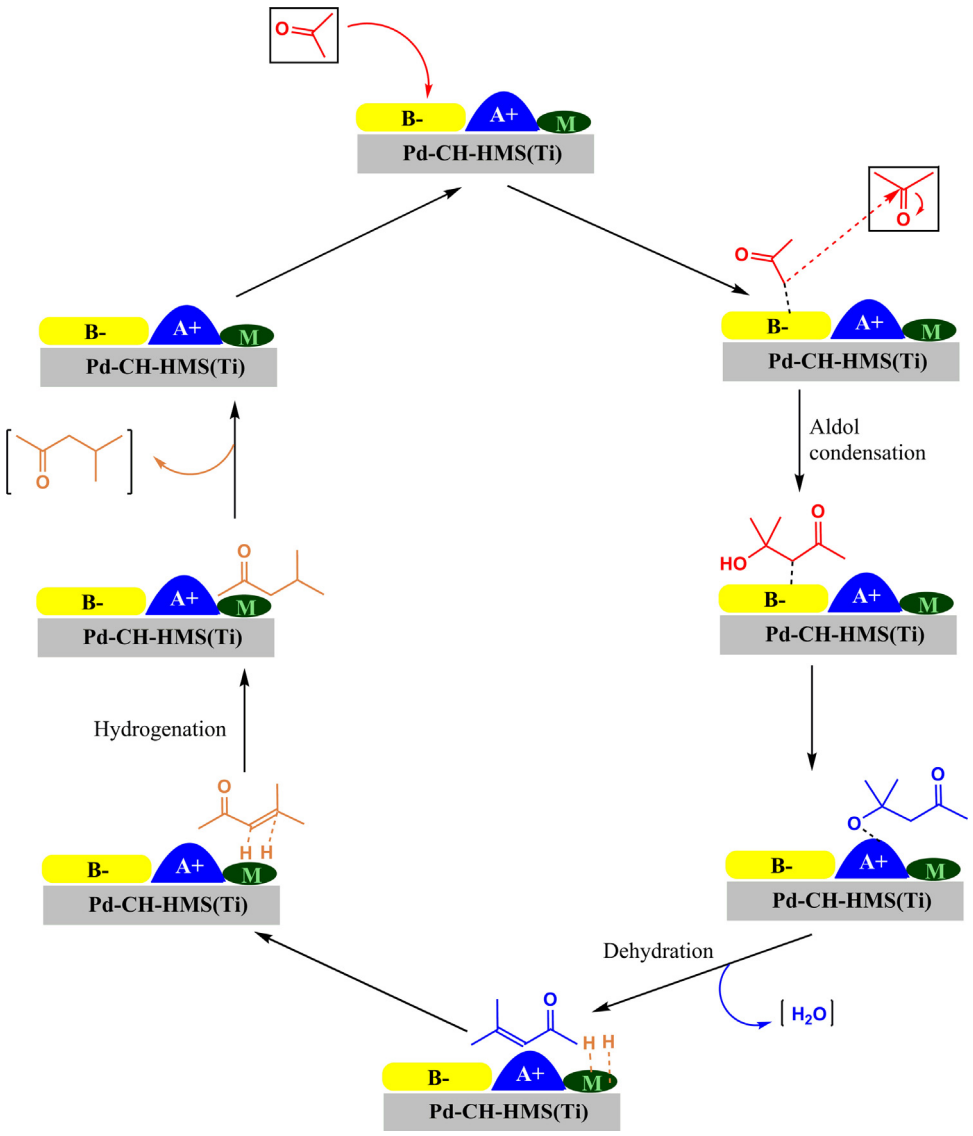

Scheme 4. Reaction mechanism for MIBK synthesis using 0.2Pd-CH(2:1)-N catalyst.

3.4.2. Effect of temperature

The effect of temperature over the rate of reaction was studied from 120 to 150 °C (Fig. ES2). The conversion was found to increase substantially with increase in temperature indicating the intrinsically kinetically controlled reaction.

3.4.3. Effect of catalyst loading

The effect of catalyst loading was studied by changing the quantity of catalyst from 0.001 to 0.003 g/cm^3 (Fig. ES3). Increase in catalyst loading increased the rate of reaction indicating the dependence of reaction on number of active sites present.

3.4.4. Activation energy and intrinsic kinetic constant calculation

A plot of $X_A/(1-X_A)$versus t was made according to equation (35) derived earlier, at different temperatures and catalyst loadings to get an excellent fit thereby supporting the model. This reaction was found to be of second order [21]. The rate constants at different temperatures were calculated and an Arrhenius plot was used to estimate the activation energy of reaction Fig. 5. The apparent activation energy was calculated to be 13.06 kcal/mol. This value proved that reaction is intrinsically kinetically controlled. The rate constants at different catalyst loadings were calculated and plotted against catalyst loading Fig. 6 to give intrinsic kinetic constant as 32.7 cm^6 mol^{-1} g_{cat}^{-1} s^{-1}.

3.5. Synthesis of MIBK from acetone using xPd-CH-N catalyst

The developed theory was extended to study a known cascade engineered synthesis involving only one starting reactant. The previous studies on one step synthesis of MIBK from acetone using palladium based heterogeneous catalysts have been summarized in Table ES3 [17–19]. Scheme 3 shows the possible reactions of acetone on 0.2Pd-CH(2:1)-N catalyst in presence of hydrogen. Acetone first adsorbs on base site to undergo aldol condensation (Reaction f). The diacetone alcohol (4-hydroxy-4-methylpentan-2-one) formed from condensation reaction then adsorbs on acid site and undergoes dehydration to form mesityl oxide (4-methylpent-3-en-2-one) (Reaction g). Later hydrogenation of mesityl oxide gives MIBK (4-methylpentan-2-one) on metal site (Reaction h). In this reaction as well, the first step of aldol condensation was found to be the rate controlling step. The parallel reaction of hydrogenation of acetone to form isopropyl alcohol (propan-2-ol) (Reaction i) becomes predominant after two hours of reaction when the concentration of acetone decreases. The other consecutive reactions

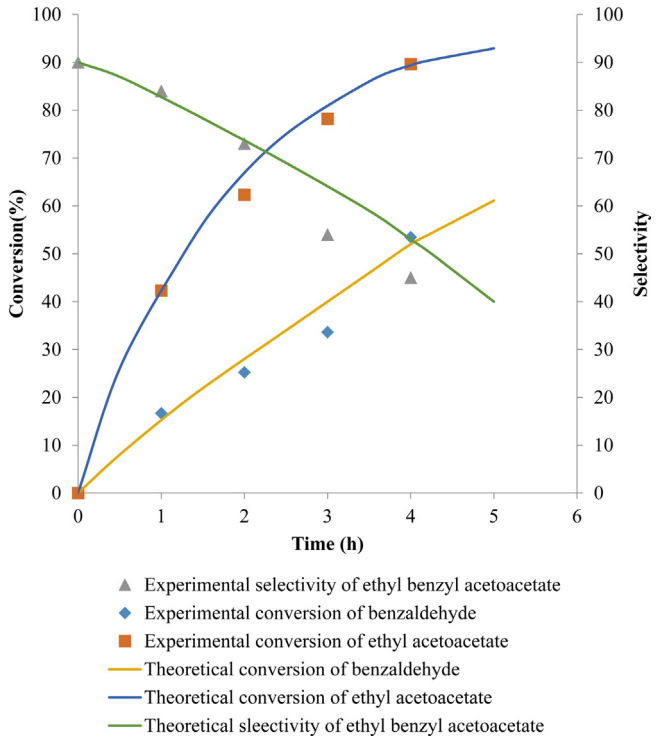

Fig. 4. Parity plot of experimental and theoretical values of conversion of ethyl acetoacetate and selectivity of ethyl benzyl acetoacetate.

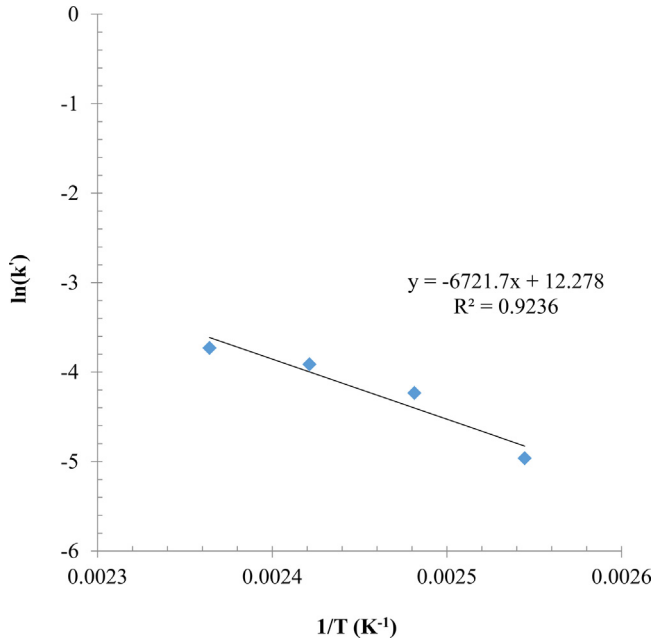

Fig. 5. Arrhenius plot of ethyl benzyl acetoacetate synthesis.

of self condensation of MIBK on acid sites to form DIBK (2,6-dimethylhept-2-en-4-one) (Reaction j) and hydrogenation of DIBK on metal sites to form DIBC (2,6-dimethylheptan-4-one) (Reaction k) were completely suppressed due to the tailored activity of catalyst with 0.2% (w/w) palladium loading. A similar derivation as ethyl benzyl acetoacetate synthesis was done for this chemistry and instantaneous selectivity equation was derived as Eq. (36).

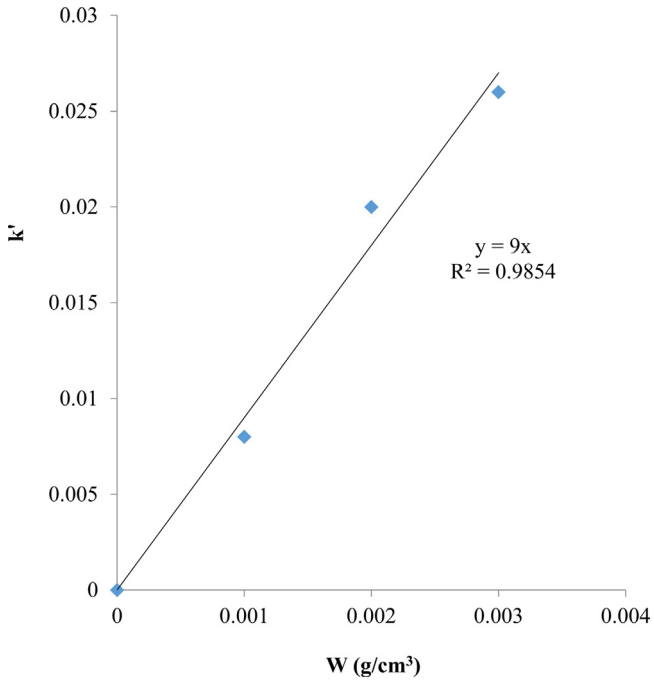

Fig. 6. Plot for intrinsic kinetic constant in ethyl benzyl acetoacetate synthesis.

Table 4
Rate and adsorption constants for MIBK synthesis.

Parameter	Step	Value
$k_{5\,(cm^3\,mol^{-1}\,s^{-1})}$	Aldol condensation reaction constant	0.23
$k_8 \times 10^4$ ($cm^3\,mol^{-1}\,s^{-1}$)	Hydrogenation reaction rate constant	1.06
$K_{I1} \times 10^5$($cm^3\,mol^{-1}$)	Adsorption constant of acetone for base site	4.88
$K_{I2} \times 10^4$($cm^3\,mol^{-1}$)	Adsorption constant of acetone for metal site	1.60
$k_E K_E \times 10^6$($cm^3\,mol^{-1}$)	Adsorption constant of hydrogen	2.62

The instantaneous selectivity is dependent on concentration of acetone and hydrogen in reaction mixture.

$$S_{L/O} = \frac{k_5 K_{I1}^2 C_I (1 + K_{I2} C_I)^2}{k_8 K_{I2} \sqrt{K_E C_E} \left(1 + K_{I1} C_I + \sqrt{K_E C_E}\right)^2} \quad (36)$$

The constants were found by interpolation (Table 4).

A plot of change in selectivity with time and comparison of theoretical values with experimental values for conversion of acetone and MIBK selectivity is shown in Fig. 7.

The reaction mechanism for synthesis of MIBK is shown pictorially in Scheme 4.

In this cascade engineered reaction to synthesize MIBK as well, hydrogen does not participate in first two reactions (Reactions f and g) and then gets utilized in third reaction (Reaction h) [22]. In the case of MIBK synthesis as well a derivation was done similar to ethyl benzyl acetoacetate synthesis. A plot of $X_I/(1 - X_I)$ versus t was made at different temperatures and catalyst loadings. After ensuring absence of mass transfer and pore diffusion resistance, experiments were done to study the effect of temperature and catalyst loading. The effect of temperature was studied over the range of 170–200 °C (Fig. ES4) and catalyst loading was studied over the range of 0.02–0.05 g/cm^3 (Fig. ES5). Activation energy was found to be 12.35 kcal/mol (Fig. ES6) and intrinsic kinetic constant as 4.50 $cm^6\,mol^{-1}\,g_{cat}{}^{-1}\,s^{-1}$ (Fig. ES7).

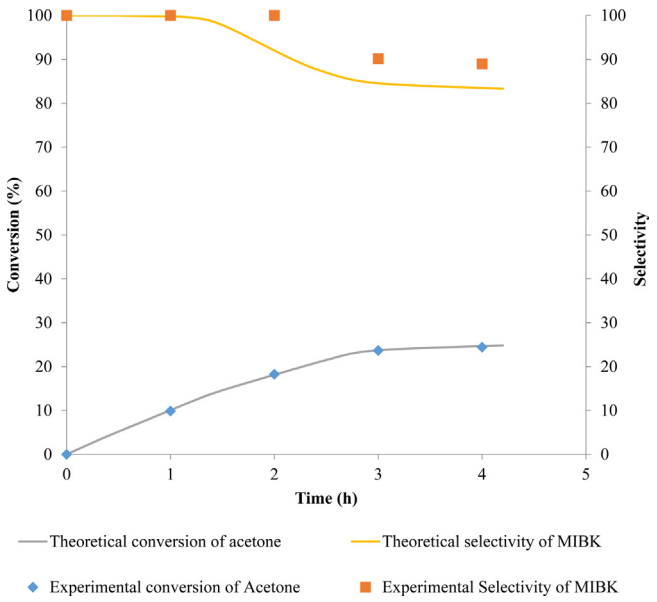

Fig. 7. Plot showing experimental and theoretical values of conversion of acetone and selectivity of MIBK.

4. Conclusion

Various catalysts were developed by impregnation, sol–gel and nanocolloidal method for studying the cascade engineered synthesis which involves condensation followed by dehydration and hydrogenation. However, xPd-CH-N was found to be the best catalyst in terms of activity and catalyst reusability. The modification of HMS with transition metal resulted in enhanced hydrogenation ability of the catalyst. The synthesized novel heterogeneous catalyst with palladium loaded on hydrtotalcite supported on titanium modified hexagonal mesoporous silica had a tunable activity. The reaction of benzaldehyde and ethyl acetoacetate involved variety of reactions happening on multifunctional catalyst. However, the reaction pathway was controlled by varying the rate of series and parallel reactions with the tunable catalyst to selectively synthesize ethyl benzyl acetoacetate. Activation energy, intrinsic kinetic constant and instantaneous selectivity were found for ethyl benzyl acetoacetate synthesis. The activity of catalyst was manipulated with basicsites > acidic sites > metal sites. However, this can be altered by changing the mole ratio of Mg:Al in hydrotalcite synthesis and by varying the loading of palladium. The catalyst was found to be reusable and robust and its fidelity was tested through characterization of the used catalyst. The extended study involving acetone as reactant showed that the catalyst was robust. Maximum selectivity of 100% was achieved for MIBK synthesis. Activation energy, intrinsic kinetic constant and instantaneous selectivity were also found for this chemistry. The catalyst can be used in a variety of chemistries with modification of active phases according to the desired reaction pathway.

Conflict of interest

The authors declare no conflict of interest.

Acknowledgements

G.D.Y. gratefully acknowledges support from R.T. Mody Distinguished Professor Endowment and J.C. Bose National Fellowship (DST, GoI). S.C.P. and S.K.D. received JRF from UGC.

Appendix A. Supplementary data

Supplementary data associated with this article can be found, in the online version, at http://dx.doi.org/10.1016/j.molcata.2015.08.018.

References

[1] C. Gabriele, S. Perathoner, Catal. Today 77 (2003) 287–297.
[2] G.D. Yadav, Y.B. Jadhav, Clean Tech. Environ. Policy 6 (2003) 32–42.
[3] G.D. Yadav, S.S. Salgaonkar, Org. Process Res. Dev. 13 (3) (2009) 501–509.
[4] W. Hoelderich, Appl. Catal. A 194–195 (2000) 487–496.
[5] K. Nicolaou, T. Montagnon, S. Snyder, Chem. Commun. (2015) 551–564.
[6] D. Tichit, M. Ortiz, D. Francova, C. Ge'rardin, B. Coq, R. Durand, F. Prinetto, G. Ghiotti, Appl. Catal. A 318 (2007) 170–177.
[7] V. Chika, A. Molnar, K. Balazsik, J. Catal. 184 (1999) 134–143.
[8] M. Climent, A. Corma, S. Iborra, M. Mifsud, J. Catal. 247 (2007) 223–230.
[9] M. Garcia, Y. Zimmermann, V. Pitchon, A. Kinnemann, Catal. Commun. 8 (2007) 400–404.
[10] K. Motokura, N. Fujita, K. Mori, T. Mizugaki, K. Ebitani, K. Kaneda, Tetra. Lett. 46 (2005) 5507–5510.
[11] A. Anan, K. Sharma, T. Asefa, J. Mol. Catal. A 288 (2008) 1–13.
[12] K. Motokura, T. Mizugaki, K. Ebitani, K. Kaneda, Tetra. Lett. 45 (2004) 6029–6032.
[13] A. G. Sharma, Design and Synthesis of Nanomaterials for Catalytic Applications, M. Chem. Eng. Thesis, Institute of Chemical Technology, Mumbai, India, 2013.
[14] S.C. Patankar, A.G. Sharma, G.D. Yadav, RSC Adv. (2015), Revised.
[15] S.C. Patankar, G.D. Yadav, ASC Sust. Chem. Eng. (2015), Revised.
[16] A. Tuel, Micropor. Mesopor. Mater. 27 (1999) 151–169.
[17] A. Nikolopoulos, B. Jang, J. Spivey, Appl. Catal. A 296 (2005) 128–136.
[18] Y. Chen, B. Liaw, H. Tan, K. Shen, Appl. Catal. A 205 (2001) 61–69.
[19] E. Kozhevnikova, I. Kozhevnikov, J. Catal. 238 (2006) 286–292.
[20] G. Armatas, C. Salmas, M. Louloudi, G. Androutsopoulos, P. Pomonis, Langmuir 19 (2003) 3128–3136.
[21] S.C. Patankar, Development of Novel Multifunctional Catalyst for Tandem Green Synthesis, M. Chem. Eng. Thesis, Institute of Chemical Technology, Mumbai, India, 2011.
[22] S.K. Dodiya, Intensification of Green Processes, M. Chem. Eng. Thesis, University of Mumbai, Mumbai, India, 2009.